



ACADEMIC
PRESS

Available online at www.sciencedirect.com

SCIENCE @ DIRECT®

Journal of Sound and Vibration 271 (2004) 757–772

JOURNAL OF
SOUND AND
VIBRATION

www.elsevier.com/locate/jsvi

Free vibrations of annular sector cantilever plates. Part 1: out-of-plane motion

Jongwon Seok*, H.F. Tiersten

*Department of Mechanical, Aerospace and Nuclear Engineering, Rensselaer Polytechnic Institute,
110 8th Street, Troy, NY 12180-3590, USA*

Received 4 June 2002; accepted 12 March 2003

Abstract

An analysis of the flexural vibrations of an annular sector plate is performed by means of a variational approximation procedure. The plate is fixed on one straight edge and free on the other three. The annular plate is assumed to have polar orthotropy in the analysis, although calculations are performed only for the isotropic case. The problem is treated by first obtaining the exact solution for flexural waves in the annular sector plate by satisfying the flexural equation of motion for the plate with the circumferential edges free. In this exact solution, new radial functions are obtained from a Fröbenius type expansion. The solution results in a set of dispersion curves. A number of the resulting waves are used in what remains of the variational equation, in which all conditions occur as natural conditions. Roots of the resulting transcendental equation are calculated, which yield the eigensolutions and associated eigenfrequencies. The results compare very well with those from FEM calculation, which shows that this procedure is very accurate. It also provides an understanding in terms of the waves that make up the vibration, which is not provided by any of the other methods.

© 2003 Elsevier Ltd. All rights reserved.

1. Introduction

The annular sector of a thin plate in flexure is an element used in many different geometric configurations. On account of this, a rather large amount of work has been done on this problem using a number of different approaches. In particular, Vogel and Skinner [1] analyzed the transverse vibrations of a plate of uniform thickness in the shape of a circular ring. Ramakrishnan and Kunukkasseril [2] solved the problem of an annular sector plate analytically for the case of simply supported radial edges and any conditions on the circumferential edges. Harik and

*Corresponding author. Tel.: +1-518-276-8003; fax: +1-518-276-8761.

E-mail address: seokj@alum.rpi.edu (J. Seok).

Molaghasemi [3] use one angular solution of the beam equation for each mode and solve the remaining radial equation for the case when the radial and circumferential edges are either simply supported or clamped in any combination. Liew and Lam [4] used the Rayleigh–Ritz method for the treatment of the flexural vibration of a not necessarily circular annular sector plate with various combinations of edge conditions. Also, several numerical or semi-numerical methods have been developed to obtain approximate solutions for the sector plate. Guruswamy and Yang [5] employed the finite element method to solve some dynamic problems of a sector plate using Mindlin plate theory [6]. Xiang et al. [7] treated the moderately thick annular sector plate problem using the Rayleigh–Ritz method. Leissa et al. [8] treated the free vibration problem of sectorial and annular sectorial plates by means of the Ritz method with two sets of admissible functions in order to accelerate the convergence. Gutiérrez et al. [9] treated a vibration problem of a polar orthotropic annular circular plate clamped or simply supported at the outer edge and free at the inner edge using the Rayleigh–Ritz method.

In this work, the problem of the flexural vibrations of the annular sector plate is treated, in which the plate is fixed on one radial edge, free on the other and free on both circumferential edges. Since this problem cannot be solved exactly, some form of approximation procedure must be employed. A variational approximation procedure is used, in which the flexural differential equation and free conditions on the two circumferential edges are satisfied exactly and the remaining free and fixed edge conditions on the radial edges are satisfied variationally. The motivation for using this procedure is to satisfy as much of the problem exactly as possible, while leaving the remainder to be satisfied variationally, using as small a number of the exact solution functions as are needed to obtain the accuracy required. The procedure is semi-analytical and provides some understanding through the values of the amplitudes of the exact solution functions used, whereas FEM and the Rayleigh–Ritz method yield only the final numbers that result. The treatment employs the variational equation for the classical theory of flexure of thin plates, in which all conditions, i.e., those of both natural and constraint types, arise as natural conditions in a form suitable for the application. The required variational equation is derived in recent work [10] on the flexural vibrations of rectangular plates. Clearly, the equations taken from Ref. [10] are in rectilinear co-ordinates and in this work the required equations must be transformed to cylindrical co-ordinates. As in the previous work, the analysis proceeds by first obtaining solutions satisfying the dynamic equation of flexure of thin plates in cylindrical co-ordinates and the free conditions on the two circumferential edges exactly. In finding these exact solutions, the radial differential equation arising is not expanded about the usual singular point, but instead is expanded about a regular point, for which the required number of independent radial power series solutions is always obtained [11]. In the particular problem occurring here, the Fröbenius form of expansion is used to obtain the independent power series solution functions directly, which are then used to satisfy the circumferential edge conditions of the intermediate problem exactly. The remaining conditions on the two radial edges and the Kirchhoff corner conditions are then satisfied variationally.

The exact solution of the differential equation and free conditions on the two circumferential edges yields dispersion curves. The dispersion curves for flexure of annular sector thin plates presented in this work are exact and, to our knowledge, have not appeared in the literature before. Up to eight of these solutions are taken, which are represented by the dispersion curves, in what remains of the variational equation with all natural conditions to obtain a system of linear

homogeneous algebraic equations, from which calculations are performed. Among other things, the calculations clearly show the dependence of the natural frequencies on the radial dimension of the plate for a given circumferential dimension. The results compare favorably with those from P3/PATRAN [12].

2. Variational equation for the out-of-plane motion of a thin orthotropic plate

Consider a fixed Cartesian co-ordinate system x_i ($i = 1, 2, 3$) with the faces, of area S , at $x_3 = \pm h$. The axes x_1 and x_2 are co-ordinates lying in the middle plane, which intersect the right prismatic boundary of the plate in a line path c . In Ref. [10], for the case of orthotropic symmetry, the variational equation for both the extension and flexure of thin plates with all conditions, i.e., both those of natural and constraint types, arising as natural conditions was obtained from the appropriate three-dimensional variational equation [13]. Since Eq. (16) of Ref. [10] shows that the extensional behavior uncouples from the flexural behavior, only the flexural behavior is treated in this work and the extensional behavior is taken to vanish here. Accordingly, from Eq. (16) of Ref. [10], the remaining flexural part of the variational equation of the plate now becomes

$$\int_{t_0}^t dt \left[\int_S dS \{ (\tau_{a3,a}^{(0)} - 2\rho h \ddot{u}_3^{(0)}) \delta u_3^{(0)} + (\tau_{ab,a}^{(1)} - \tau_{3b}^{(0)}) \delta u_b^{(1)} \} \right. \\ \left. + \int_{c_C} ds \{ u_3^{(0)} \delta (n_a \tau_{a3}^{(0)}) - u_{3,b}^{(0)} \delta (n_a \tau_{ab}^{(1)}) \} \right. \\ \left. - \int_{c_N} ds \{ (n_a \tau_{a3}^{(0)} + (n_a \tau_{ab}^{(1)} s_b)_{,s}) \delta u_3^{(0)} - n_a \tau_{ab}^{(1)} n_b \delta u_{3,n}^{(0)} \} + \int_{c_N} ds (n_a \tau_{ab}^{(1)} s_b \delta u_{3,s}^{(0)}) \right] = 0, \quad (1a)$$

where indicial notation has been introduced and the conventions have been employed that a comma followed by an index denotes partial differentiation with respect to the spatial co-ordinate indicated by the index, a dot over a variable denotes partial differentiation with respect to time and repeated tensor indices are to be summed, and as in Ref. [10] the convention that a, b can take the values 1 and 2 but not 3 has been used. In this equation, the symbols S and ρ stand for the area and the mass density of the plate, respectively, the subscripts n, s after commas represent the spatial derivatives along the normal and tangential directions of the edges, respectively, c_N stands for the portion of edges on which traction is prescribed and c_C represents the portion of edges on which mechanical displacement is prescribed, n_a, s_b denote the components of the unit outward normal vector and the unit tangent vector to the curve of the edge in the counterclockwise direction, respectively. In this equation, the n th order components of the stress-resultants are defined by

$$\tau_{ij}^{(n)} = \int_{-h}^h \tau_{ij} x_3^n dx_3 \quad (1b)$$

and the n th order components of mechanical displacement are defined by the relations

$$u_b = \sum_{n=0}^1 x_3^n u_b^{(n)}(x_a, t), \quad u_3 = \sum_{n=0}^2 x_3^n u_3^{(n)}(x_a, t), \quad (1c)$$

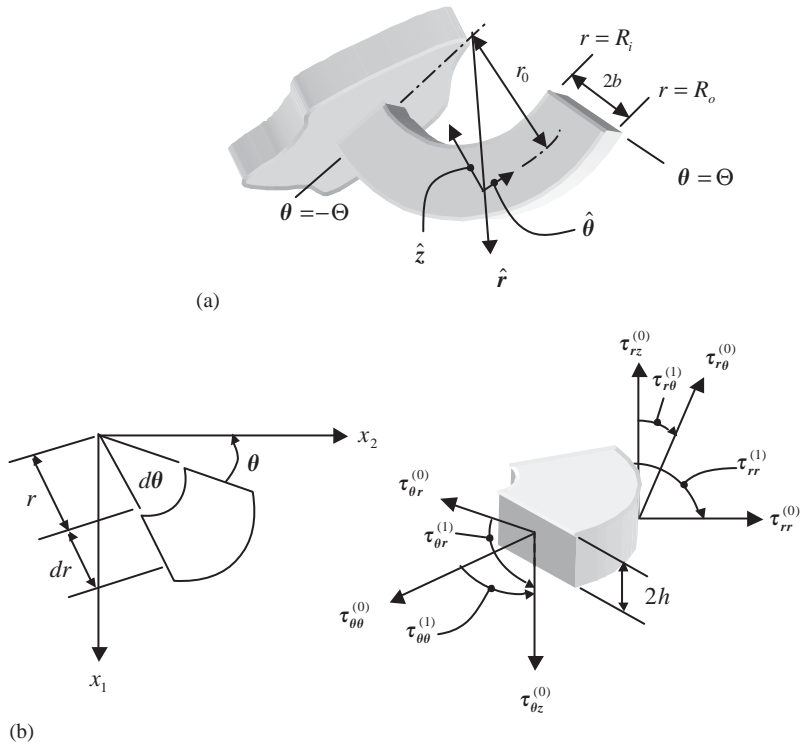


Fig. 1. Three-dimensional view of an annular sector cantilever plate and its plan view of an element with stress resultants and co-ordinates: (a) three-dimensional view of the annular sector cantilever plate, (b) an element of the annular sector plate.

Table 1
Compressed matrix notation scheme

<i>ij</i> or <i>kl</i>	11	22	33	23 (or 32)	31 (or 13)	12 (or 21)
<i>p</i> or <i>q</i>	1	2	3	4	5	6

where τ_{ij} and u_j denote the components of the stress tensor and mechanical displacement vector, respectively, and the time integration has been ignored since it is not needed in this work. Note that all of the inhomogeneous terms in Eq. (1a) have been ignored since they are not required in this treatment and that all of the assumptions of classical flexure discussed in Ref. [10] have been employed.

Now, consider an annular sector plate and its co-ordinate system shown in Fig. 1(a). In the figure, a cylindrical co-ordinate system with unit vectors \hat{r} , $\hat{\theta}$, \hat{z} is adopted to describe the flexural motion of the plate. Fig. 1(b) represents an element of the annular sector plate showing the relevant stress resultants required in the description of both flexure and extension of the plate.

With the aid of the compressed matrix notation given in Table 1, in which the tensor indices 1, 2, 3 correspond to r, θ, z for the cylindrical co-ordinate system, the linear constitutive equation

can be expressed in the compact form [14]

$$\tau_p = c_{pq}\varepsilon_q, \tag{2a}$$

where $c_{pq} \triangleq c_{ijkl}$ are the elastic stiffnesses, ε_{kl} denote the components of strain and

$$\tau_p \triangleq \tau_{ij}, \quad \begin{cases} \varepsilon_q \triangleq \varepsilon_{kl} & \text{for } q = 1, 2, 3, \\ \varepsilon_q \triangleq 2\varepsilon_{kl} & \text{for } q = 4, 5, 6. \end{cases}$$

For a polar orthotropic material, the constitutive relations can be represented in the matrix form

$$\begin{bmatrix} \tau_1 \\ \tau_2 \\ \tau_3 \\ \tau_4 \\ \tau_5 \\ \tau_6 \end{bmatrix} = \begin{bmatrix} c_{11} & c_{12} & c_{13} & 0 & 0 & 0 \\ c_{21} & c_{22} & c_{23} & 0 & 0 & 0 \\ c_{31} & c_{32} & c_{33} & 0 & 0 & 0 \\ 0 & 0 & 0 & c_{44} & 0 & 0 \\ 0 & 0 & 0 & 0 & c_{55} & 0 \\ 0 & 0 & 0 & 0 & 0 & c_{66} \end{bmatrix} \begin{bmatrix} \varepsilon_1 \\ \varepsilon_2 \\ \varepsilon_3 \\ \varepsilon_4 \\ \varepsilon_5 \\ \varepsilon_6 \end{bmatrix}. \tag{2b}$$

From the development of the thin plate equations in Section 2 of Ref. [10], the two-dimensional constitutive equations for flexure in cylindrical co-ordinates can be obtained in the form

$$[\tau_1^{(1)}, \tau_2^{(1)}, \tau_6^{(1)}] = \hat{\Theta}^{(1,1)} [c_{11}^*\varepsilon_1^{(1)} + c_{12}^*\varepsilon_2^{(1)}, c_{12}^*\varepsilon_1^{(1)} + c_{22}^*\varepsilon_2^{(1)}, c_{66}\varepsilon_6^{(1)}], \tag{3}$$

where

$$\varepsilon_1^{(1)} = -\frac{\partial^2 u_3^{(0)}}{\partial r^2}, \quad \varepsilon_2^{(1)} = -\frac{1}{r} \frac{\partial u_3^{(0)}}{\partial r} - \frac{1}{r^2} \frac{\partial^2 u_3^{(0)}}{\partial \theta^2}, \quad \varepsilon_6^{(1)} = -\frac{1}{r} \frac{\partial^2 u_3^{(0)}}{\partial r \partial \theta} + \frac{1}{r^2} \frac{\partial u_3^{(0)}}{\partial \theta} \tag{4}$$

are the components of the two-dimensional plate strain in cylindrical co-ordinates for the flexural behavior of the plate and the plate shearing strains $\varepsilon_{3a}^{(0)}$ have already been taken to vanish, which results in Eq. (11) below, as required for classical flexure [15] and

$$c_{11}^* = c_{11} - c_{13}^2/c_{33}, \quad c_{12}^* = c_{12} - c_{13}c_{32}/c_{33}, \quad c_{22}^* = c_{22} - c_{23}^2/c_{33} \tag{5}$$

are the two-dimensional, or plate, polar orthotropic elastic constants.

The transformation of the variational equation (1a) to the cylindrical co-ordinate system with the aid of the definition of the tensor indices 1, 2, 3 given above Eq. (2a) enables

us to write

$$\begin{aligned}
 & \int_S dS \left[\left\{ \frac{\partial \tau_{rz}^{(0)}}{\partial r} + \frac{1}{r} \left(\frac{\partial \tau_{\theta z}^{(0)}}{\partial \theta} + \tau_{rz}^{(0)} \right) - 2\rho h \ddot{w} \right\} \delta w \right. \\
 & + \left. \left\{ \frac{\partial \tau_{rr}^{(1)}}{\partial r} + \frac{1}{r} \frac{\partial \tau_{r\theta}^{(1)}}{\partial \theta} + \frac{(\tau_{rr}^{(1)} - \tau_{\theta\theta}^{(1)})}{r} - \tau_{rz}^{(0)} \right\} \delta u_r^{(1)} \right. \\
 & + \left. \left\{ \frac{\partial \tau_{r\theta}^{(1)}}{\partial r} + \frac{1}{r} \left(\frac{\partial \tau_{\theta\theta}^{(1)}}{\partial \theta} + 2\tau_{r\theta}^{(1)} \right) - \tau_{\theta z}^{(0)} \right\} \delta u_\theta^{(1)} \right] \\
 & - \int_{-\theta}^{\theta} \left[r \left\{ \left(\tau_{rz}^{(0)} + \frac{1}{r} \frac{\partial \tau_{r\theta}^{(1)}}{\partial \theta} \right) \delta w - \tau_{rr}^{(1)} \delta \left(\frac{\partial w}{\partial r} \right) \right\} \right]_{r=R_i}^{r=R_o} d\theta \\
 & - \int_{R_i}^{R_o} \left[w \delta \tau_{\theta z}^{(0)} - \frac{\partial w}{\partial r} \delta \tau_{r\theta}^{(1)} \right]_{\theta=-\theta} d r - \int_{R_i}^{R_o} \left[\left(\tau_{\theta z}^{(0)} + \frac{\partial \tau_{\theta r}^{(1)}}{\partial r} \right) \delta w - \tau_{\theta\theta}^{(1)} \delta \left(\frac{1}{r} \frac{\partial w}{\partial \theta} \right) \right]_{\theta=\theta} d r \\
 & - [\tau_{r\theta}^{(1)} \delta w]_{r=R_i, \theta=-\theta}^{r=R_o, \theta=-\theta} + 2[\tau_{r\theta}^{(1)} \delta w]_{r=R_i, \theta=\theta}^{r=R_o, \theta=\theta} = 0, \tag{6}
 \end{aligned}$$

where the time integration has been omitted since it is not needed in this work. For convenience, the symbol $u_3^{(0)}$ has been replaced by w , and the definitions

$$[f(x)]_{x=a}^{x=b} = f(b) - f(a), \quad [g(x)]_{x=c} = g(c) \tag{7}$$

have already been employed.

Note that the last two terms in Eq. (6) were obtained by performing the last line integral around c_N in Eq. (1a) along the three free edges in the counterclockwise direction. The first of these in Eq. (6) arises from the integration along the two opposite free edges evaluated at the wall and the second and last of these came from the two jump conditions across the edges of discontinuity, which are given by

$$- \llbracket n_a \tau_{ab}^{(1)} s_b \delta w \rrbracket_{x_1=R_i, x_2=\theta} - \llbracket n_a \tau_{ab}^{(1)} s_b \delta w \rrbracket_{x_1=R_o, x_2=\theta}, \tag{8}$$

and the jump notation

$$\llbracket p(x) \rrbracket_{x=q} \quad \text{for } p^+(q) - p^-(q)$$

has been introduced.

As discussed in Ref. [10], since in the formulation the constraint conditions were included by the method of Lagrange multipliers, each variation is treated as independent, the coefficient of each variation in Eq. (6) must vanish, which yields the differential equation and edge conditions. However, since the resulting equations cannot be solved exactly, the intermediate problem of satisfying the differential equation and edge conditions on the two circumferential edges exactly is treated first. This solution yields dispersion curves giving frequency vs. wavenumber in the θ direction relations. In the next section, the dispersion relations for the flexural motion of the annular sector plate are obtained.

At this point it should be noted that although we have provided in Fig. 1(b) a differential element of the plate in cylindrical co-ordinates containing all the relevant stress resultants, we do not derive the flexural and extensional differential equations from the element, but instead derive

the differential equations systematically from the variational formulation. This is done because although we solve much of the problem exactly, we ultimately leave a portion to be satisfied variationally and, consequently, we feel that the discourse will be clearer if all the equations and conditions that are satisfied exactly are obtained from the basic variational equation. Accordingly, since all the variations δw , $\delta u_r^{(1)}$ and $\delta u_\theta^{(1)}$ in the surface integral in Eq. (6) are independent,

$$\frac{\partial \tau_{rz}^{(0)}}{\partial r} + \frac{1}{r} \left(\frac{\partial \tau_{\theta z}^{(0)}}{\partial \theta} + \tau_{rz}^{(0)} \right) - 2\rho h \ddot{w} = 0, \tag{9a}$$

$$\frac{\partial \tau_{rr}^{(1)}}{\partial r} + \frac{1}{r} \frac{\partial \tau_{r\theta}^{(1)}}{\partial \theta} + \frac{(\tau_{rr}^{(1)} - \tau_{\theta\theta}^{(1)})}{r} - \tau_{rz}^{(0)} = 0, \tag{9b}$$

$$\frac{\partial \tau_{r\theta}^{(1)}}{\partial r} + \frac{1}{r} \left(\frac{\partial \tau_{\theta\theta}^{(1)}}{\partial \theta} + 2\tau_{r\theta}^{(1)} \right) - \tau_{\theta z}^{(0)} = 0 \tag{9c}$$

are obtained.

Since for the elementary flexure of thin plates the wavelength along the plate is much larger than the thickness, the constitutive equations for $\tau_{rz}^{(0)}$ and $\tau_{\theta z}^{(0)}$ may be ignored and Eq. (9b) and Eq. (9c) are to be used instead. The substitution of Eq. (9b) and Eq. (9c) into Eq. (9a) yields the classical form of the differential equation for the flexural vibrations of a thin plate in cylindrical co-ordinates in the form

$$\frac{\partial^2 \tau_{rr}^{(1)}}{\partial r^2} + \frac{2}{r} \frac{\partial^2 \tau_{r\theta}^{(1)}}{\partial r \partial \theta} + \frac{1}{r^2} \frac{\partial^2 \tau_{\theta\theta}^{(1)}}{\partial \theta^2} + \frac{2}{r^2} \frac{\partial \tau_{r\theta}^{(1)}}{\partial \theta} + \frac{2}{r} \frac{\partial \tau_{rr}^{(1)}}{\partial r} - \frac{1}{r} \frac{\partial \tau_{\theta\theta}^{(1)}}{\partial r} = 2\rho h \ddot{w}. \tag{10}$$

Since Mindlin’s condition [15] of vanishing vertical plate shearing strains has already been employed, there results

$$u_r^{(1)} = -\frac{\partial w}{\partial r}, \quad u_\theta^{(1)} = -\frac{1}{r} \frac{\partial w}{\partial \theta}, \tag{11}$$

which yields one differential equation, i.e., Eq. (10), in one variable w , i.e., the deflection. Since the variations δw and $\delta(\partial w/\partial r)$ along the traction-free circumferential edges are independent, the two edge conditions

$$\tau_{rr}^{(1)} = 0, \quad \tau_{rz}^{(0)} + \frac{1}{r} \frac{\partial \tau_{r\theta}^{(1)}}{\partial \theta} = 0 \tag{12}$$

at $r = R_i$ and $r = R_0$ are obtained.

For the polar orthotropic material, the two-dimensional constitutive equations (3) and the strain-displacement relations (4) yield the two-dimensional bending and twisting moment-displacement gradient relations

$$\tau_{rr}^{(1)} = -\hat{D} \left\{ \frac{\partial^2 w}{\partial r^2} + \frac{\hat{\nu}}{r} \left(\frac{\partial w}{\partial r} + \frac{1}{r} \frac{\partial^2 w}{\partial \theta^2} \right) \right\}, \tag{13}$$

$$\tau_{\theta\theta}^{(1)} = -\hat{D} \left\{ \hat{\nu} \frac{\partial^2 w}{\partial r^2} + \frac{R}{r} \left(\frac{\partial w}{\partial r} + \frac{1}{r} \frac{\partial^2 w}{\partial \theta^2} \right) \right\}, \tag{14}$$

$$\tau_{r\theta}^{(1)} = -\hat{D}(T - \hat{\nu})\frac{\partial^2}{\partial r\partial\theta}\left(\frac{w}{r}\right), \tag{15}$$

where

$$\hat{D} = 2h^3 c_{11}^*/3, \quad \hat{\nu} = c_{12}^*/c_{11}^*, \quad T = (2c_{66}/c_{11}^*) + \hat{\nu}, \quad R = c_{22}^*/c_{11}^*. \tag{16}$$

For a transversely isotropic material, where the $r - \theta$ co-ordinates define the plane of isotropy, the stress resultant-displacement gradient relations may readily be obtained from those for the polar orthotropic material simply by setting $T = R = 1$.

The substitution of Eqs. (13)–(15) into Eqs. (9b) and (9c) yields the vertical shear-displacement gradient relations in the form

$$\tau_{rz}^{(0)} = -\hat{D}\left\{\frac{1}{r}\frac{\partial}{\partial r}\left(r\frac{\partial^2 w}{\partial r^2}\right) + \frac{T}{r}\frac{\partial^3}{\partial\theta^2\partial r}\left(\frac{w}{r}\right) - \frac{R}{r^2}\left(\frac{\partial w}{\partial r} + \frac{1}{r}\frac{\partial^2 w}{\partial\theta^2}\right)\right\}, \tag{17}$$

$$\tau_{\theta z}^{(0)} = -\hat{D}\frac{\partial}{\partial\theta}\left\{\frac{T}{r}\frac{\partial^2 w}{\partial r^2} + \frac{R}{r^2}\left(\frac{\partial w}{\partial r} + \frac{1}{r}\frac{\partial^2 w}{\partial\theta^2}\right)\right\}, \tag{18}$$

which, with Eq. (15), result in

$$\tau_{rz}^{(0)} + \frac{1}{r}\frac{\partial\tau_{r\theta}^{(1)}}{\partial\theta} = -\hat{D}\left\{\frac{\partial^3 w}{\partial r^3} - \frac{R}{r^2}\frac{\partial w}{\partial r} + \frac{1}{r}\frac{\partial^2 w}{\partial r^2} - \frac{R}{r^3}\frac{\partial^2 w}{\partial\theta^2} + \frac{(2T - \hat{\nu})}{r^2}\left(\frac{\partial^3 w}{\partial r\partial\theta^2} - \frac{1}{r}\frac{\partial^2 w}{\partial\theta^2}\right)\right\}, \tag{19}$$

$$\begin{aligned} \tau_{\theta z}^{(0)} + \frac{\partial\tau_{\theta r}^{(1)}}{\partial r} = & -\hat{D}\left\{\frac{R}{r^3}\frac{\partial^3 w}{\partial\theta^3} - \frac{(2T - R)}{r^2}\frac{\partial^2 w}{\partial r\partial\theta} + \frac{2T}{r}\left(\frac{\partial^3 w}{\partial r^2\partial\theta} + \frac{1}{r^2}\frac{\partial w}{\partial\theta}\right) \right. \\ & \left. - \hat{\nu}\left(\frac{1}{r}\frac{\partial^3 w}{\partial r^2\partial\theta} + \frac{2}{r^3}\frac{\partial w}{\partial\theta} - \frac{2}{r^2}\frac{\partial^2 w}{\partial r\partial\theta}\right)\right\}. \end{aligned} \tag{20}$$

It should be noted that the effective flexural rigidity \hat{D} and Poisson’s ratio $\hat{\nu}$ in the two-dimensional stress resultant-displacement gradient relations with $T = R = 1$ become, respectively, the flexural rigidity D and Poisson’s ratio ν for an isotropic plate.

3. Solution of the differential equation and edge conditions on the two traction-free circumferential faces

The substitution of Eqs. (13)–(15) into Eq. (10) yields the differential equation for the flexural motion of the polar orthotropic plate in the form

$$\begin{aligned} & \frac{1}{r^2}\frac{\partial}{\partial r}\left(r^2\frac{\partial^3 w}{\partial r^3}\right) + \frac{2T}{r^2}\frac{\partial^3}{\partial r\partial\theta^2}\left(\frac{\partial w}{\partial r} - \frac{w}{r}\right) \\ & + \frac{R}{r}\left\{\frac{1}{r^3}\frac{\partial^2}{\partial\theta^2}\left(\frac{\partial^2 w}{\partial\theta^2} + 2w\right) - \frac{\partial}{\partial r}\left(\frac{1}{r}\frac{\partial w}{\partial r}\right)\right\} + \hat{\kappa}^2\ddot{w} = 0, \end{aligned} \tag{21}$$

where

$$\hat{\kappa} = \sqrt{2\rho h/\hat{D}}. \tag{22}$$

From Eq. (12), the free edge conditions at $r = R_i, R_o$ are given by

$$\tau_{rr}^{(1)} = 0, \quad \tau_{rz}^{(0)} + \frac{1}{r} \frac{\partial \tau_{r\theta}^{(1)}}{\partial \theta} = 0. \tag{23}$$

As a solution of Eq. (21), write

$$w(r, \theta, t) = \Re\{\tilde{w}(r)e^{i(\omega t - \xi\theta)}\}, \tag{24}$$

where $i = \sqrt{-1}$, and the symbol $\Re\{\}$ signifies the real part of the argument and will be dropped hereafter.

The substitution of Eq. (24) into the differential equation (21) yields

$$\begin{aligned} \tilde{w}'''' + \frac{2}{r}\tilde{w}''' - \frac{(2T\xi^2 + R)}{r^2}\tilde{w}'' + \frac{(2T\xi^2 + R)}{r^3}\tilde{w}' \\ + \left[\frac{R\xi^2}{r^4}\{\xi^2 - 2(T + R)\} - \hat{\kappa}^2\omega^2 \right] \tilde{w} = 0, \end{aligned} \tag{25}$$

where the superscript prime ($'$) means the derivative with respect to r . A new series representation of the solutions of Eq. (25) is now obtained in this work. Since the existence of the singular point at $r = 0$ in Eq. (25) causes numerous convergence problems in the series solutions of Eq. (25), series solutions are obtained about a point other than $r = 0$, for which it is known [11] that expansion about a regular point of the fourth order differential equation (25) with variable coefficients yields four independent exact power series solutions about that point, which are well behaved in the region of interest. In particular, the point r_0 in the center of the annulus is particularly convenient for use in this work.

For the purpose of calculation, it is convenient to introduce dimensionless quantities, which are defined by

$$\bar{r} = \pi r / (2b), \quad \bar{r}_0 = \pi r_0 / (2b), \quad \tilde{r} = \bar{r} - \bar{r}_0, \tag{26}$$

$$\bar{\kappa} = \hat{\kappa}\bar{\omega}(2b/\pi)^2, \quad \bar{\Omega} = \omega/\bar{\omega}, \quad \tau = \bar{\omega}t, \tag{27}$$

where

$$b = \frac{R_o - R_i}{2}, \quad \bar{\omega} = \frac{\pi}{2b} \sqrt{\frac{c_{66}}{\rho}}. \tag{28}$$

Eq. (25) now takes the dimensionless form

$$\begin{aligned} (\tilde{r} + \bar{r}_0)^4 \tilde{w}'''' + 2(\tilde{r} + \bar{r}_0)^3 \tilde{w}''' - (\tilde{r} + \bar{r}_0)^2 (2T\xi^2 + R) \tilde{w}'' + (\tilde{r} + \bar{r}_0) (2T\xi^2 + R) \tilde{w}' \\ + [R\xi^2\{\xi^2 - 2(T + R)\} - (\tilde{r} + \bar{r}_0)^4 \bar{\kappa}^2 \bar{\Omega}^2] \tilde{w} = 0, \end{aligned} \tag{29}$$

where the superscript prime ($'$) means the derivative with respect to dimensionless radius \tilde{r} .

Four independent solutions of Eq. (29) are now sought in order to satisfy the four edge conditions given in Eq. (23) along with the substitution of Eqs. (13), (15) and (17). The most convenient way of obtaining the four independent solutions is to introduce the Fröbenius form [16]

$$\tilde{w}(\tilde{r}) = \sum_{m=0}^{\infty} \tilde{\alpha}_m \tilde{r}^{\lambda+m}, \tag{30}$$

where the $\bar{\alpha}_m$ represent the m th coefficients of $\tilde{r}^{\lambda+m}$ and λ represents characteristic numbers to be determined. Note that in the above equation, the function $\tilde{w}(r)$ was directly replaced by a new function $\tilde{w}(\tilde{r})$, which, for corresponding points r and \tilde{r} have the same values as the former function, and for the sake of simplicity are denoted by the same symbols.

The insertion of Eq. (30) in Eq. (29) and the collection of the coefficients of like powers of \tilde{r} yields the recursion relations for all the solutions, which are much too cumbersome to include. The coefficient of $\tilde{r}^{\lambda-4}$, which is the lowest power term, yields the indicial equation in the form

$$\bar{r}_0^4 \bar{\alpha}_0 \lambda(\lambda - 1)(\lambda - 2)(\lambda - 3) = 0. \tag{31}$$

Clearly, Eq. (31) guarantees the existence of four independent solutions in the form of power series for $\bar{\alpha}_0 \neq 0$. The solutions are denoted by $\lambda_{(q)} = q - 1$, $q = 1, \dots, 4$. Consequently, four independent solutions are obtained, which may be written in the form

$$G_q(\tilde{r}; \xi) = \sum_{m=0}^M \bar{\alpha}_m^{(q)}(\xi) \tilde{r}^{\lambda_{(q)}+m}, \quad q = 1, \dots, 4, \tag{32}$$

where the $\bar{\alpha}_m^{(q)}$ ($m \neq 0$) are determined in terms of $\bar{\alpha}_0^{(q)} = 1$ from the recursion relations and

$$\bar{\alpha}_m^{(q)} = \bar{\alpha}_m(\lambda_{(q)}) \tag{33}$$

and M is an integer large enough to make the four series solutions converge in the region of interest.

With the aid of Eqs. (13) and (19), and the introduction of the dimensionless variables defined in Eq. (26), it is found that the four edge conditions in Eq. (23) may be written in the form

$$(\tilde{r} + \bar{r}_0)^2 \tilde{w}'' + \hat{\nu} \{(\tilde{r} + \bar{r}_0) \tilde{w}' - \xi^2 \tilde{w}\} = 0, \quad \text{at } \tilde{r} = \pm \pi/2, \tag{34}$$

$$\begin{aligned} &(\tilde{r} + \bar{r}_0) \{(\tilde{r} + \bar{r}_0)^2 \tilde{w}''' + (\tilde{r} + \bar{r}_0) \tilde{w}'' - R \tilde{w}'\} \\ &+ \xi^2 \{ (2T + R - \hat{\nu}) \tilde{w} - (2T - \hat{\nu})(\tilde{r} + \bar{r}_0) \tilde{w}' \} = 0, \quad \text{at } \tilde{r} = \pm \pi/2. \end{aligned} \tag{35}$$

In accordance with the foregoing, as a solution of Eqs. (34) and (35), take

$$\tilde{w}(\tilde{r}; \xi) = \sum_{q=1}^4 A_q G_q. \tag{36}$$

The substitution of Eq. (36) into Eqs. (34) and (35) yields four homogeneous equations with four unknowns A_q , which can be written in the form

$$\sum_{q=1}^4 [[(\tilde{r} + \bar{r}_0)^2 G_q'' + \hat{\nu} \{(\tilde{r} + \bar{r}_0) G_q' - \xi^2 G_q\}] A_q] = 0, \quad \text{at } \tilde{r} = \pm \pi/2, \tag{37}$$

$$\begin{aligned} &\sum_{q=1}^4 [[(\tilde{r} + \bar{r}_0) \{(\tilde{r} + \bar{r}_0)^2 G_q''' + (\tilde{r} + \bar{r}_0) G_q'' - R G_q'\} \\ &+ \xi^2 \{ (2T + R - \hat{\nu}) G_q - (2T - \hat{\nu})(\tilde{r} + \bar{r}_0) G_q' \}] A_q] = 0, \quad \text{at } \tilde{r} = \pm \pi/2, \end{aligned} \tag{38}$$

which result in

$$\sum_{q=1}^4 L_{pq} A_q = 0, \quad p = 1, \dots, 4, \tag{39}$$

where $p = 1, 2$ refers to the two edge conditions in Eq. (37) and $p = 3, 4$ refers to the two edge conditions in Eq. (38). Clearly, in matrix notation, Eq. (39) may be written in the form

$$\mathbf{L}\mathbf{A} = \mathbf{0}. \tag{40}$$

The vanishing of the determinant of matrix \mathbf{L} gives the dispersion relations, which connect the θ -directional wavenumber ξ to the circular frequency $\bar{\Omega}$, and the amplitude ratios for any solution point on the dispersion curves may be obtained from any three of the consistent homogeneous equations in Eq. (40). It should be noted that the waves of the plate are asymmetric in the annular case.

The starting points of the dispersion curves can be easily calculated by letting $\xi = 0$ in Eq. (25) and the two free boundary conditions in Eqs. (34) and (35). In that case, the governing differential equation (25) reduces to the form

$$\frac{1}{r^2} \frac{\partial}{\partial r} \left(r^2 \frac{\partial^3 \tilde{w}}{\partial r^3} \right) - \frac{R}{r} \frac{\partial}{\partial r} \left(\frac{1}{r} \frac{\partial \tilde{w}}{\partial r} \right) - \hat{\kappa}^2 \omega^2 \tilde{w} = 0. \tag{41}$$

Note that $R = T = 1$ for the material with hexagonal symmetry, and even for that case, four independent solutions are always obtained from the fourth order differential equation in Eq. (29), which insures the satisfaction of the four circumferential edge conditions in Eqs. (34) and (35).

4. Variational approximation

Since the solution function (36) satisfies the differential equation (29) and the edge conditions (34) and (35) exactly, all that remains in the variational equation (6) is

$$\begin{aligned} & - \int_{R_i}^{R_o} \left[\left[\left(\tau_{\theta z}^{(0)} + \frac{\partial \tau_{\theta r}^{(1)}}{\partial r} \right) \delta w - \tau_{\theta \theta}^{(1)} \delta \left(\frac{1}{r} \frac{\partial w}{\partial \theta} \right) \right]_{\theta=\theta} + \left[w \delta \tau_{\theta z}^{(0)} - \frac{\partial w}{\partial r} \delta \tau_{r \theta}^{(1)} \right]_{\theta=-\theta} \right] dr \\ & - [\tau_{r \theta}^{(1)} \delta w]_{r=R_o, \theta=-\theta}^{r=R_o, \theta=\theta} + 2[\tau_{r \theta}^{(1)} \delta w]_{r=R_i, \theta=\theta}^{r=R_i, \theta=-\theta} = 0. \end{aligned} \tag{42}$$

The substitution of Eqs. (9c), (13)–(15) and (20) into Eq. (42) along with the dimensionless quantities defined in Eqs. (26)–(28) yields

$$\begin{aligned} & \int_{-\pi/2}^{\pi/2} d\tilde{r} \left[\frac{1}{(\tilde{r} + \bar{r}_0)} \frac{\partial}{\partial \theta} \left[\left\{ \frac{1}{(\tilde{r} + \bar{r}_0)^2} \left(2T w + R \frac{\partial^2 w}{\partial \theta^2} \right) + 2T \frac{\partial^2 w}{\partial \tilde{r}^2} - \frac{(2T - R)}{(\tilde{r} + \bar{r}_0)} \frac{\partial w}{\partial \tilde{r}} \right\} \right. \right. \\ & \left. \left. - \hat{v} \left\{ \frac{2w}{(\tilde{r} + \bar{r}_0)^2} + (\tilde{r} + \bar{r}_0)^2 \frac{\partial}{\partial \tilde{r}} \left(\frac{1}{(\tilde{r} + \bar{r}_0)^2} \frac{\partial w}{\partial \tilde{r}} \right) \right\} \delta w \right] \end{aligned}$$

$$\begin{aligned}
 & - \left\{ \frac{R}{(\tilde{r} + \bar{r}_0)} \left(\frac{1}{(\tilde{r} + \bar{r}_0)^2} \frac{\partial^2 w}{\partial \theta^2} + \frac{1}{(\tilde{r} + \bar{r}_0)} \frac{\partial w}{\partial \tilde{r}} \right) + \frac{\hat{v}}{(\tilde{r} + \bar{r}_0)} \frac{\partial^2 w}{\partial \tilde{r}^2} \right\} \delta \left(\frac{\partial w}{\partial \theta} \right) \Big|_{\theta=\Theta} \\
 & + \int_{-\pi/2}^{\pi/2} d\tilde{r} \left[w \delta \left\{ \frac{1}{(\tilde{r} + \bar{r}_0)} \frac{\partial}{\partial \theta} \left(\frac{R}{(\tilde{r} + \bar{r}_0)^2} \frac{\partial^2 w}{\partial \theta^2} + \frac{R}{(\tilde{r} + \bar{r}_0)} \frac{\partial w}{\partial \tilde{r}} + T \frac{\partial^2 w}{\partial \tilde{r}^2} \right) \right\} \right. \\
 & \left. - (T - \hat{v}) \frac{\partial w}{\partial \tilde{r}} \delta \left\{ \frac{1}{(\tilde{r} + \bar{r}_0)} \frac{\partial}{\partial \theta} \left(\frac{\partial w}{\partial \tilde{r}} - \frac{w}{(\tilde{r} + \bar{r}_0)} \right) \right\} \right]_{\theta=-\Theta} \\
 & + (T - \hat{v}) \left[\frac{\partial^2}{\partial \tilde{r} \partial \theta} \left\{ \frac{w}{(\tilde{r} + \bar{r}_0)} \right\} \right]_{\tilde{r}=-\pi/2, \theta=-\Theta}^{\tilde{r}=\pi/2, \theta=-\Theta} - 2(T - \hat{v}) \left[\frac{\partial^2}{\partial \tilde{r} \partial \theta} \left\{ \frac{w}{(\tilde{r} + \bar{r}_0)} \right\} \right]_{\tilde{r}=-\pi/2, \theta=\Theta}^{\tilde{r}=\pi/2, \theta=\Theta} = 0. \quad (43)
 \end{aligned}$$

From Eqs. (24) and (36) when N dispersion curves are included it is clear that the solution function can be written in the form

$$w(\tilde{r}, \theta, \tau) = \sum_{n=1}^N \sum_{p=1}^4 \sum_{q=1}^2 B_{nq} \bar{A}_{pn} G_p^{(n)} \sin\{\xi_n \theta + (q - 1)\pi/2\} e^{i\bar{\Omega}\tau}, \quad (44)$$

where

$$G_p^{(n)} = G_p(\xi_n), \quad \bar{A}_{pn} = \bar{A}_p(\xi_n). \quad (45)$$

Note that for a complex component in B_{nq} , its complex conjugate should also be included.

The introduction of the solution function (44) into Eq. (43) yields a homogeneous linear algebraic system consisting of $2N$ equations with $2N$ unknowns, which may be written in the matrix form

$$\mathbf{K}\mathbf{X} = \mathbf{0}, \quad (46)$$

where \mathbf{K} is a $2N \times 2N$ matrix and \mathbf{X} is a $2N$ unknown column vector with the relation

$$B_{nq} = X_{2(n-1)+q}. \quad (47)$$

The vanishing of the determinant of \mathbf{K} yields the transcendental characteristic equation for the annular sector cantilever plate and the amplitude ratios from any $2N - 1$ of the consistent equations. The amplitude ratios in Eq. (47) along with the solution function (44) give the mode shapes of the annular sector plate.

5. Discussion of results

The calculation was performed using Maple [17] with quadruple precision and 20 significant digits, with which the branches having large imaginary parts of the wavenumbers can be handled with sufficient accuracy. Even though all the equations are derived for a polar orthotropic material,¹ the numerical computation was performed for a material with hexagonal symmetry in which the symmetry axis is normal to the plane of the plate, so that $T = R = 1$. Since the material

¹The analysis is performed for a polar orthotropic material because the solution for that symmetry is required in future work.

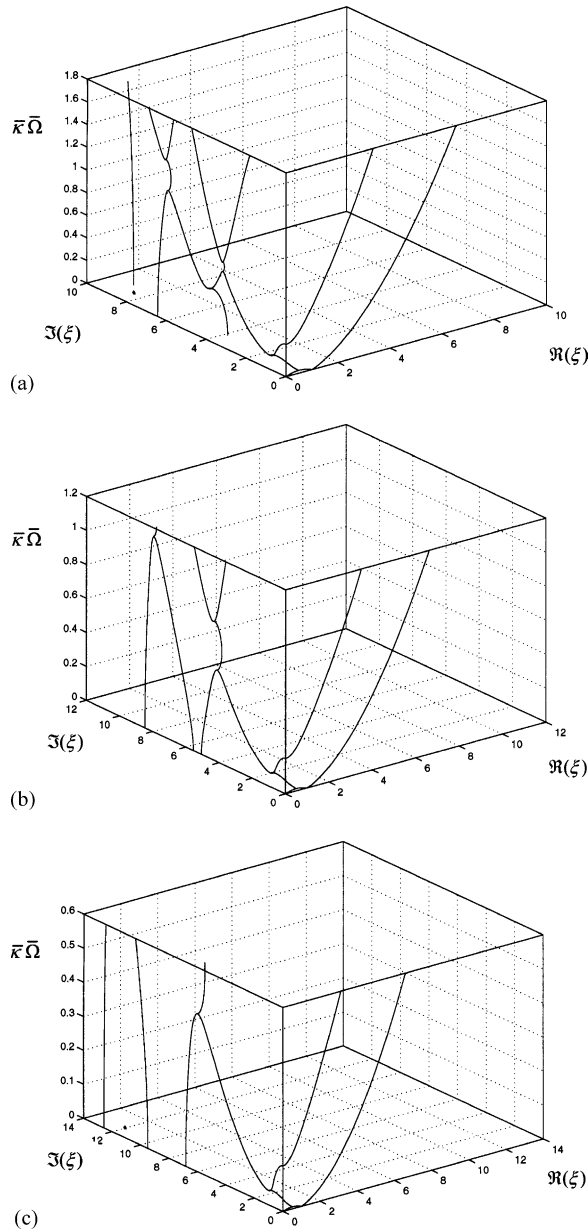


Fig. 2. Dispersion curves of the annular sector cantilever plate ($r_0 = (R_o + R_i)/2$, $b = (R_o - R_i)/2$): (a) for $r_0/2b = 5/4$, (b) for $r_0/2b = 5/3$, (c) for $r_0/2b = 5/2$.

is transversely isotropic, only the effective Poisson’s ratio and the geometry have an influence on the results. In the calculation, the effective Poisson’s ratio $\hat{\nu} = 0.35$ was used. Since the dispersion curves in the proper wavenumber range are required before the eigenmodes given in Section 4 can be calculated, the dispersion curves naturally were calculated first, and are shown in Fig. 2. Since

Table 2

Dimensionless natural frequencies for the out-of-plane motion of the annular sector cantilever plate and their comparison with P3/PATRAN [12] ($r_0 = (R_o + R_i)/2$, $b = (R_o - R_i)/2$, $N(\cdot)$ = Natural frequency $\bar{\kappa}\bar{\Omega}$ (ND) of (\cdot)); C_n (ND) = N (current research) with n dispersion branches included P (ND) = N (P3/PATRAN)

Mode #	2Θ (rad)											
	$\pi/4$		$\pi/2$		$3\pi/4$		π		$5\pi/4$		$3\pi/2$	
$r_0/(2b) = 5/4$												
1	C_6	0.34112	C_6	0.09906	C_6	0.05083	C_6	0.03322	C_6	0.02464	C_6	0.01973
	P	0.34839	P	0.10004	P	0.05108	P	0.03319	P	0.02472	P	0.01987
2	C_6	1.01344	C_6	0.34067	C_6	0.14987	C_6	0.07977	C_6	0.04934	C_6	0.03455
	P	1.01691	P	0.34603	P	0.15254	P	0.08074	P	0.04967	P	0.03460
3	C_8	1.71872	C_6	0.60422	C_6	0.37628	C_6	0.24312	C_6	0.15116	C_6	0.09726
	P	1.72310	P	0.60732	P	0.37663	P	0.24481	P	0.15207	P	0.09792
$r_0/(2b) = 5/3$												
1	C_5	0.20117	C_5	0.05575	C_5	0.02799	C_5	0.01805	C_5	0.01331	C_5	0.01066
	P	0.20524	P	0.05614	P	0.02807	P	0.01801	P	0.01337	P	0.01069
2	C_5	0.64877	C_5	0.21193	C_5	0.08981	C_5	0.04667	C_5	0.02839	C_5	0.01960
	P	0.65013	P	0.21450	P	0.09097	P	0.04714	P	0.02860	P	0.01960
3	C_6	1.11117	C_5	0.38847	C_5	0.24359	C_5	0.14794	C_5	0.08912	C_5	0.05629
	P	1.11225	P	0.38929	P	0.24364	P	0.14830	P	0.08964	P	0.05654
$r_0/(2b) = 5/2$												
1	C_5	0.09080	C_5	0.02449	C_5	0.01213	C_5	0.00777	C_5	0.00571	C_5	0.00418
	P	0.09180	C_5	0.02466	P	0.01218	P	0.00777	P	0.00571	P	0.00417
2	C_5	0.36684	C_5	0.10487	C_5	0.04212	C_5	0.02138	C_5	0.01281	C_5	0.00875
	P	0.36840	P	0.10593	P	0.04249	P	0.02154	P	0.01289	P	0.00877
3	C_5	0.55557	C_5	0.21910	C_5	0.12916	C_5	0.07045	C_5	0.04120	C_5	0.02562
	P	0.55671	P	0.21951	P	0.12947	P	0.07062	P	0.04137	P	0.02572

two dimensions are required to locate the circumferential portions of the annular sector plate, the dispersion curves depend on a dimensional ratio in addition to Poisson’s ratio. The figure shows the dispersion relations for the three values $r_0/(2b) = 5/4, 5/3$ and $5/2$, which are needed for our further calculations. In this figure, the dimensionless frequency $\bar{\kappa}\bar{\Omega}$ is plotted against $\Re(\xi)$ and $\Im(\xi)$ over a range that includes the first three imaginary (or complex) branches near $\bar{\Omega} = 0$. Here, $\Re(\xi)$ and $\Im(\xi)$ represent real and imaginary, respectively. Note that a complex branch depicted in Fig. 2 always represents two branches since its complex conjugate is also a branch. Therefore, whenever the number of branch is mentioned, a complex branches is counted twice.

The natural frequencies calculated for the first three modes of the cantilevered annular sector plate using the treatment presented in this work are shown in Table 2 along with a comparison with those obtained from the P3/PATRAN [12] calculation. For the FEM, around 800 to 1200 quadrilateral elements were employed depending on the geometry of the plate, and the subspace iteration method [12] was also used. As can be seen from the table, the results are in very good agreement, especially for large angles, and hence, for low frequencies. The limitation on the number of the branches included naturally causes a reduction in accuracy, which should become

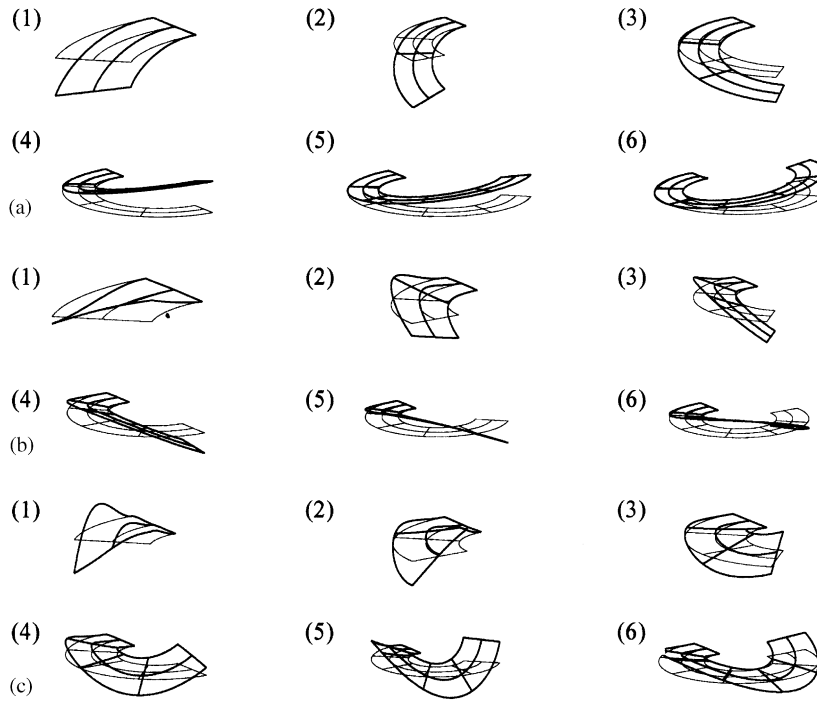


Fig. 3. First six mode shapes for the out-of-plane motion of the annular sector cantilever plate [(1), ..., (6) correspond to $2\theta = n\pi/4$, $n = 1, \dots, 6$]: (a) first modes for $r_0/(2b) = 5/4$, (b) second modes for $r_0/(2b) = 5/3$, (c) third modes for $r_0/(2b) = 5/2$.

larger as the frequency gets higher. Of course, this accuracy can readily be improved simply by including more branches.

Fig. 3 shows the first three mode shapes of the annular sector cantilever plate with various angles between the two ends of the sector (2θ) and three dimensionless ratios $r_0/(2b)$.

References

- [1] G.M. Vogel, D.W. Skinner, Natural frequencies of transversely vibrating uniform annular plates, *Journal of Applied Mechanics* 32 (4) (1965) 926–931.
- [2] R. Ramakrishnan, V.X. Kunukkasseril, Free vibration of annular sector plate, *Journal of Sound and Vibration* 30 (1) (1973) 127–129.
- [3] I.E. Harik, H.R. Molaghasemi, Analytic solution to free vibration of sector plates, *Journal of Engineering Mechanics* 115 (1989) 2709–2722.
- [4] K.M. Liew, K.Y. Lam, On the use of 2-D orthogonal polynomials in the Rayleigh–Ritz method for flexural vibration of annular sector plates of arbitrary shape, *International Journal of Mechanical Sciences* 35 (2) (1993) 129–139.
- [5] P. Guruswamy, T.Y. Yang, A sector finite element for dynamic analysis of thick plates, *Journal of Sound and Vibration* 62 (4) (1979) 505–516.
- [6] R.D. Mindlin, An introduction to the mathematical theory of the vibration of elastic plates, US Army Signal Corps Engineering Laboratory, Fort Monmouth, NJ, 1955, Sec. 5.06.

- [7] Y. Xiang, K.M. Liew, S. Kitipornchai, Transverse vibration of thick annular sector plates, *Journal of Engineering Mechanics* 119 (8) (1993) 1579–1597.
- [8] A.W. Leissa, O.G. McGee, C.S. Huang, Vibrations of sectorial plates having corner stress singularities, *Journal of Applied Mechanics* 60 (1993) 134–140.
- [9] R.H. Gutiérrez, P.A.A. Laura, D. Félix, C. Pistonesi, Fundamental frequency of transverse vibration of circular, annular plates of polar orthotropy, *Journal of Sound and Vibration* 230 (5) (2000) 1191–1195.
- [10] Jongwon Seok, H.F. Tiersten, H.A. Scarton, Free vibrations of rectangular cantilever plates. Part 2: in-plane motion, *Journal of Sound and Vibration* 271 (3–5) (2004) 773–787, [this issue](#).
- [11] P.M. Morse, H. Feshbach, *Methods of Theoretical Physics*, McGraw-Hill, New York, 1953, Part I, pp. 530–531.
- [12] P3/PATRAN™ User Manual Release 1.2, PDA Engineering-PATRAN Division, 1993.
- [13] H.F. Tiersten, *Linear Piezoelectric Plate Vibrations*, Plenum Press, New York, 1969, Sec. 6.4 (6.44) without the electrical terms and the integral over $S^{(d)}$, since it is for only one region.
- [14] H.F. Tiersten, *Linear Piezoelectric Plate Vibrations*, Plenum Press, New York, 1969, Sec. 7.1.
- [15] R.D. Mindlin, *An introduction to the mathematical theory of the vibration of elastic plates*, US Army Signal Corps Engineering Laboratory, Fort Monmouth, NJ, 1955, Sec. 6.04.
- [16] F.B. Hildebrand, *Advanced Calculus for Applications*, Prentice-Hall, Englewood Cliffs, NJ, 1976, Sec. 4.4.
- [17] Maple™ User Manual Release 5, Waterloo Maple Inc., 1997.